Traveling-wave relaxation in elongated liquid crystal cells

R. H. Self,* C. P. Please,† and T. J. Sluckin‡

Southampton Liquid Crystal Institute and Faculty of Mathematical Studies, University of Southampton, Southampton SO17 1BJ, United Kingdom

(Received 30 June 1999)

We have made a theoretical study of Freedericksz relaxation in a long thin nematic liquid crystal cell subject to strong anchoring on the short ends and weak anchoring on the long sides. On removing an imposed magnetic field, three different types of relaxation behavior may be observed. Two of these are simple generalizations of one-dimensional relaxation channels, and are dominated by either the ends or the sides. The third is a traveling wave, nucleated by the strong anchoring ends of the cell but driven by the weak anchoring sides and is the result of a subtle balance between the two classical mechanisms. A phase diagram is derived, identifying the relaxation regimes as a function of the nondimensional initial field and the anchoring strength in the long cell limit. A comparison is made between numerical results and a simple one-dimensional theory derived from an asymptotic analysis. Surprisingly, the traveling wave behavior occurs for a large region of parameter space. [S1063-651X(99)50211-0]

PACS number(s): 64.70.Md, 61.30.−v, 05.45.Yv

The search for more efficient liquid crystal devices has led to intense study of novel geometries [1]. In a simple cell, the aligning mechanism involves a balance between the bulk field and the elastic energy required to rotate the director over the width of the cell from the boundary-imposed orientation to that favored by the bulk [2]. By contrast, the aligning process in the more complicated geometries can be more complex, in that the relevant length scales involve combinations of the sample size and characteristic pore sizes.

In this paper we discuss the Freedericksz transition in one such nonclassical geometry that exhibits interesting realignment mechanisms. In particular, we find that the alignment process upon removal of the external field can involve slow invasion of the sample by a wave produced by the boundary-imposed orientation, rather than the usual diffusion process in which realignment takes place through the growth of a bulk reorientation Fourier mode. This solitonlike reorientation should be contrasted with other instances of soliton and solitonlike reorientation in liquid crystals, which almost universally involve reorientation in an external field, rather than on removal of the external field [3].

The cell geometry is shown in Fig. 1. Whereas the conventional Freedericksz geometry involves a cell homogeneous in two dimensions, and with dimension d in a third dimension, this geometry involves only one infinite (x) dimension. There are now two relevant directions: a thick cell dimension (z) of length of d and a thin cell dimension (y) of length l, where we shall consider $l/d \ll 1$. In addition, the face normal to the long dimension has strong anchoring conditions (which we shall take to be perpendicular to this face), whereas the face normal to the short dimension imposes only weak anchoring in the same direction, with the weak anchoring characterized by a strength W [4].

For simplicity, we shall assume the one constant approximation in which the elastic constants $K=K_{11}=K_{33}$. The only relevant angle is θ, which defines the director orientation with respect to the z axis, so that $\hat{\mathbf{n}}=(0,\sin\theta,\cos\theta)$. We shall assume an external magnetic field H, so as to avoid complications with a self-consistent Poisson equation, with negative dielectric anisotropy that rotates the director in a direction perpendicular to itself. The director remains nevertheless in the yz plane.

The free energy, per unit length in the x direction, is now given by

$$\mathcal{F}=\frac{1}{2}\int_{-d/2}^{d/2} dz\, W \sin^2\theta(\pm d/2,z) + \frac{1}{2}\int_{-d/2}^{d/2} dz \int_{-l/2}^{l/2} dy\,(K(\nabla\theta)^2-\Delta\chi H^2\sin^2\theta). \quad (1)$$

The presence of the weak anchoring introduces a length scale $\zeta=K/W$. Strong anchoring shrinks the extrapolation length ζ to zero, whereas weak anchoring expands ζ to macroscopic length scales.

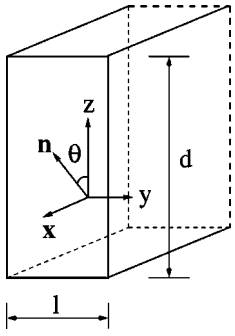

FIG. 1. Cell geometry.

*Present address: Institute of Sound and Vibration Research, University of Southampton, Southampton SO17 1BJ, United Kingdom. Electronic address: rhs@maths.soton.ac.uk

†Electronic address: cpp@maths.soton.ac.uk

‡Electronic address: tjs@maths.soton.ac.uk

This complex geometry consists, in some sense, of a superposition of a one-dimensional conventional strong anchoring cell of length d (Freedericksz field H_1) and a weak anchoring cell of length l (Freedericksz field H_1'). These threshold fields are well known:

$$H_1^2=\frac{K\pi^2}{\Delta\chi d^2};\quad H_1'^2=2\frac{W}{\Delta\chi l}. \tag{2}$$

We now discuss equilibrium and relaxation to equilibrium when the applied field H is removed. The governing equations are

$$K\left(\frac{\partial^2\theta}{\partial z^2}+\frac{\partial^2\theta}{\partial y^2}\right)+\Delta\chi H^2\sin\theta\cos\theta=\gamma_1\frac{\partial\theta}{\partial t}, \tag{3a}$$

$$\theta\left(y,\pm\frac{d}{2}\right)=0, \tag{3b}$$

$$K\frac{\partial\theta}{\partial y}\left(\pm\frac{l}{2},z\right)=\mp W\sin\theta\cos\theta, \tag{3c}$$

where γ_1 is the rotational viscosity [5]. Here backflow, which often accompanies liquid crystal reorientation, is suppressed by the close proximity of no-slip surfaces in the thin direction and hence has been neglected.

We introduce nondimensional parameters

$$h=\frac{H}{H_1},\quad w=\frac{d^2}{l\zeta}=\frac{Wd^2}{lK},\quad \epsilon=\frac{l}{d} \tag{4}$$

and nondimensional variables

$$T=\frac{K}{\gamma_1 d^2}t,\quad Z=\frac{z}{d}\quad Y=\frac{y}{l}. \tag{5}$$

The problem can now be rewritten as

$$\theta_{ZZ}+\frac{1}{\epsilon^2}\theta_{YY}+\pi^2h^2\sin\theta\cos\theta=\theta_T, \tag{6a}$$

$$\theta(Y,\pm\tfrac{1}{2})=0, \tag{6b}$$

$$\theta_Y(\pm\tfrac{1}{2},Z)=\mp\epsilon^2 w\sin\theta\cos\theta. \tag{6c}$$

The Freedericksz field h_c can be calculated by examining the linear stability of the $\theta=0$ state, and is given by

$$q\tan\frac{q}{2}=\epsilon^2 w, \tag{7}$$

where $q^2=\epsilon^2\pi^2(h_c^2-1)$. This can be linearized to yield

$$h_c^2=1+\frac{2w}{\pi^2}, \tag{8}$$

corresponding to the formula $H_c^2=H_1^2+H_1'^2$, with H_1,H_1' defined in Eq. (2).

It will also turn out to be useful to examine the stability of the uniform state $\theta=\pi/2$. This is the *saturated* state, which cannot occur in this cell but could occur in a cell without strong anchoring ends. If we ignore the Z derivative in Eq. (6a), we obtain an implicit formula for the saturation field h_{sat}:

$$\pi h_{sat}\epsilon\tanh\left(\frac{1}{2}\pi h_{sat}\epsilon\right)=\epsilon^2 w. \tag{9}$$

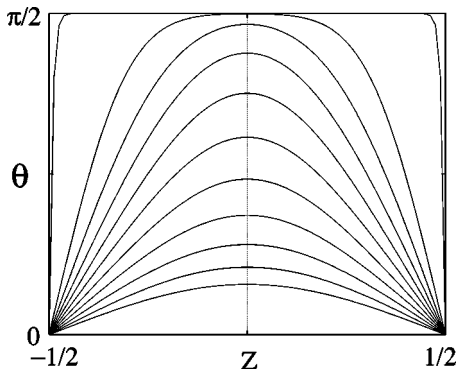

FIG. 2. Type I (diffusive) reorientation in the case $\epsilon=0.025$, $w=10$, $h=14.96$, showing $\theta(Y=0,Z)$ for $T=0.0$ to $T=0.1$ in steps of 0.001.

The formulas (7),(9) for the Freedericksz and the saturation fields can be compared. In the limit of small ϵ, the difference between these two quantities is $O(\epsilon^2)$, and is thus small.

We now move on to the process of relaxation to equilibrium following the removal of the nondimensional field h. The relevant control parameters are the applied field h, the anchoring w, and the cell aspect ratio ϵ. We assume that $h>h_c$, where h_c which depends on ϵ and w is the Freedericksz threshold, in order that we have some distortion to relax from. In the cases we discuss we shall restrict ourselves to the physically interesting regime of $\epsilon\ll 1$ and find that the qualitative features of the relaxation behavior are then largely independent of ϵ. We first discuss the results of numerical studies of Eqs. (6).

For very weak anchoring (w small) the behavior is dominated by reorientation from the hard anchoring boundaries, as would occur in a one-dimensional cell of width d. This is usually known as diffusive relaxation, which we denote as type I relaxation and is illustrated in Fig. 2 by θ for $Y=0$ at fixed time intervals. Note that the behavior at other values of Y is essentially indistinguishable. For large initial fields the initial, nearly uniform, θ relaxes first to a sinelike shape, which is the principal mode, and this then relaxes exponentially.

If the weak anchoring is much stronger (w large) it is necessary to impose a large field h to create an initial distortion. Relaxation now takes place more uniformly over the cell with the strong anchoring boundaries affecting only a small local region. The behavior is, as expected, similar to a cell of width l with weak anchoring. We refer to this as type II relaxation and its structure is shown in Fig. 3.

The most interesting, and novel, behavior occurs when there is significant anchoring (w large) and a very large initial field is applied (h large). In this case the initial distortion effectively saturates the weak anchoring (note that the strong

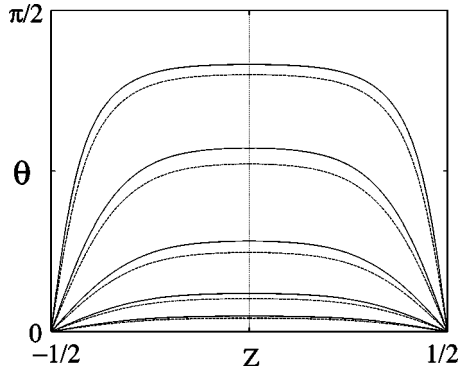

FIG. 3. Type II (spatially uniform) reorientation in the case $\epsilon = 0.025$, $w = 1000$, $h = 14.96$, showing $\theta(Y = 0, Z)$ (solid line) and $\theta(Y = 0.5, Z)$ (dotted line) for $T = 0.0$, 0.005, 0.0015, 0.002.

anchoring surfaces prevent complete saturation). In this case the relaxation takes place through a wave-of-invasion mechanism, outlined in Fig. 4. The surface-aligned region invades the field-aligned region. The walls $Z = \pm 1/2$ act as nucleation sites for the $\theta = 0$ region, which invades the $\theta = \pi/2$ region. The fronts are almost uniform in the Y direction and move at an essentially constant speed in the Z direction. Finally, the two fronts collide in the middle of the cell, rapidly eliminating the $\theta = \pi/2$ region. We refer to this behavior as type III relaxation.

Where these three different types of behavior occur in (h, w) parameter space (for $\epsilon = 0.025$) can be summarized in a phase diagram, which we show in Fig. 5.

Additional insight can be found by considering an asymptotic analysis of the problem in the limit $\epsilon \ll 1$. Taking this limit in Eqs. (6) indicates that the solution must basically depend on Z alone. Hence we shall therefore solve for the variable $\overline{\theta}$, which is the leading order term in an expansion in ϵ:

$$\theta(Y, Z) = \overline{\theta}(Z) + \epsilon^2 \theta_2(Y, Z) + \cdots . \tag{10}$$

In this case, changes in orientation along the very thin Y direction of the cell are energetically unfavorable and hence are very small.

In order to derive an equation for $\overline{\theta}$, first substitute the assumed expansion (10) into (6a) and consider the resulting leading order, $O(\epsilon^0)$, equation

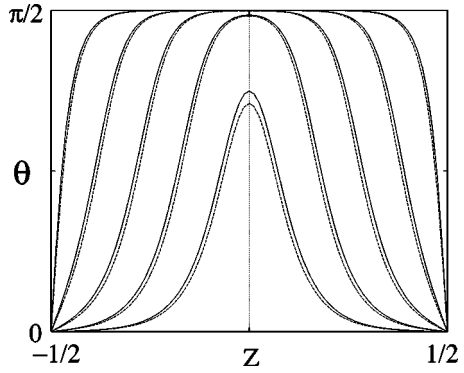

FIG. 4. Type III (traveling wave) reorientation in the case $\epsilon = 0.025$, $w = 1000$, $h = 17.51$, showing $\theta(Y = 0, Z)$ (solid line) and $\theta(Y = 0.5, Z)$ (dotted line) for $T = 0.0$, 0.01, 0.02, 0.03, 0.04.

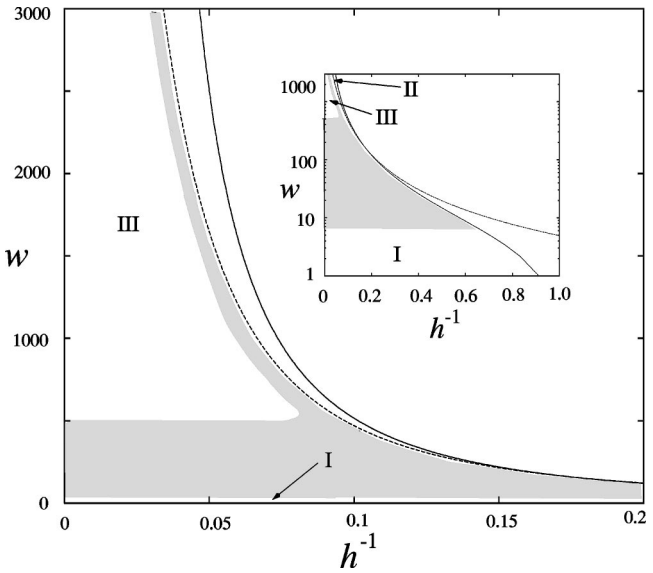

FIG. 5. Phase diagram showing regions with different relaxation types for $\epsilon = 0.025$. Inset shows a larger range of h^{-1}. In each case the field in the region to the right of the solid line is below the Freedericksz threshold [calculated from Eq. (7)], while the dotted line [from Eq. (9)] indicates the saturation field. Shaded regions as discussed in text.

$$\overline{\theta}_{ZZ} + \theta_{2YY} + \pi^2 h^2 \sin\overline{\theta}\cos\overline{\theta} - \overline{\theta}_T = 0. \tag{11}$$

The dependency on θ_2 can be removed by integrating this equation with respect to Y to give

$$\int_{-1/2}^{1/2} dY(\overline{\theta}_{ZZ} + \theta_{2YY} + \pi^2 h^2 \sin\overline{\theta}\cos\overline{\theta} - \overline{\theta}_T) = 0. \tag{12}$$

The terms in this integral involving $\overline{\theta}$ have no Y dependence and so are trivial while for the remaining term we have

$$\int_{-1/2}^{1/2} dY(\theta_{2YY}) = \theta_{2Y}(\tfrac{1}{2}, Z) - \theta_{2Y}(-\tfrac{1}{2}, Z) = -2w \sin\overline{\theta}\cos\overline{\theta}, \tag{13}$$

where we have used the boundary conditions (6c). Hence the problem for $\overline{\theta}$ becomes

$$\overline{\theta}_{ZZ} + (\pi^2 h^2 - 2w)\sin\overline{\theta}\cos\overline{\theta} = \overline{\theta}_T, \tag{14}$$

$$\text{subject to} \quad \overline{\theta} = 0 \quad \text{at} \quad Z = \pm\tfrac{1}{2}. \tag{15}$$

Equation (14) is a Fisher-Kolmogorov-type equation [6] that can sustain traveling-wave solutions. Physically, the weak surface anchoring has been averaged over the whole width of the cell to create an effective field on the average orientation.

We now explore solutions to Eqs. (14), (15) when the external field h, which has been present for a long time and created an initial equilibrium configuration, is suddenly removed. The type of relaxation that then occurs depends on the relative sizes of w and h.

Analysis shows that when $h = 0$ the slowest and narrowest traveling-wave solution of Eq. (14), in an infinite region, has

in scaled units a velocity of $2w^{1/2}$ and a wave thickness proportional to $w^{-1/2}$. Hence, if we have $w \leqslant O(1)$ then the wave cannot fit in the cell length. Reorientation then occurs through the growth of reorientational fluctuations, driven by Fick's law. This diffusional reorientation time, in scaled units, is $T_D \sim O(1)$, yielding $t_D \sim \bar{\gamma} d^2/K$. This is type I behavior.

For large values of w the wave is short enough to fit in the cell; however, there may not be sufficient time for it to develop. This development time depends on the initial shape of the distortion and hence on h. For fields larger than h_c, but not too large, the wave cannot develop because the averaged weak anchoring term reorients the field in a time scale of $T_R \sim w^{-1}$. This behavior corresponds to type II relaxation. In contrast, if the initial field is very large $h \gg w$, then over most of the cell the distortion is nearly saturated. In this case the weak-anchoring driven reorientation time is very long. The boundary conditions at $z = \pm 1/2$ are able to nucleate the reorientation, resulting in a traveling wave and a time scale of $T_R \sim w^{-1/2}$ which we identify with type III behavior.

The asymptotic analysis gives expressions for the boundaries between the various behaviors. These boundaries are: (i) the classical Freedericksz transition when distortion first appears, (ii) the saturation boundary where the weak anchoring is overcome, and (iii) the boundary where a traveling wave can no longer fit in the cell. The analytical expressions for these boundaries are given in Eqs. (7), (9) and are shown as lines in Fig. 5. The numerical results have also been considered and interpreted so that the different behavior is identified.

The shaded regions in the figure indicate where the behavior is in transition and not of any single type. Because of the different scales involved, the main part of Fig. 5 uses a linear w plot to show the II/III transition while the insert uses a logarithm w scale to better indicate the I/II transition. Note that the I/II transition region is rather wide but the II/III transition region is very sharp. In fact, the latter becomes much sharper as the aspect ratio ϵ becomes smaller. This agrees with the earlier discussion following Eq. (9). We also note that the size of the spatially uniform relaxation type II regime diminishes as ϵ is reduced. One of the significant observations to make concerning Fig. 5 is that the region of (h,w) parameter space where traveling-wave behavior occurs is much larger than might be expected.

In conclusion, we have examined the reorientation process following removal of a field in a complex cell with strongly anchored ends and weakly anchored sides. We find three relaxation regimes. In the weak-anchoring limit, the relaxation is organized by the *ends* of the cell, and takes place on a time scale $t_1 \sim \bar{\gamma} d^2/K$. For weak-ordering fields, the relaxation is organized by the *sides* of the cell, and takes place on a time scale $t_2 \sim \bar{\gamma} l/K$. These are simply generalizations of the relevant simple Freedericksz cell relaxation. For initially strong ordering fields, the relaxation takes place through a compromise between these mechanisms. This is a wave of advance, nucleated at the ends of the cell but driven by the sides, with relaxation time $t_3 \sim \bar{\gamma} d l^{1/2}/(KW)^{1/2} \sim (t_1 t_2)^{1/2}$. Fuller details of all calculations can be found in [7].

R.H.S. thanks the Faculty of Mathematical Studies for financial support during the course of this work.

[1] See, e.g., *Liquid Crystals in Complex Geometries Formed by Polymer and Porous Networks*, edited by G.P. Crawford and S. Žumer (Taylor and Francis, London, 1996).

[2] P.G. de Gennes and J. Prost, *The Physics of Liquid Crystals* (Oxford University Press, Oxford, 1993).

[3] *Solitons in Liquid Crystals*, edited by L. Lam and J. Prost (Springer-Verlag, New York, 1991).

[4] A. Rapini and M. Papoular, J. Phys. (Paris) **30**, C4-54 (1969).

[5] The effect of a surface viscosity, as employed, e.g., by J. Stelzer, R. Hirning, and H.-R. Trebin, J. Appl. Phys. **74**, 6046 (1993) can easily be included.

[6] See, e.g., D. Zwillinger, *Handbook of Differential Equations* (Academic Press, London, 1992).

[7] R.H. Self, Ph.D. thesis, University of Southampton, UK, 1998 (unpublished).